Modeling and interpretation of CSEM data from Bressay, Bentley and Kraken area of East Shetland Platform, North Sea

Anwar Bhuiyan, Rune Sakariassen, Øystein Hallanger and Allan McKay, PGS*

Summary

The heavy oil reservoirs of the Bentley, Bressay and Kraken (BBK) of East Shetland Platform (ESP) are in close proximity to other highly resistive layers such as the regional Balder Tuff that lies directly above the reservoirs, and a granite intrusion that sits beneath the Bentley discovery. The subsurface geology is complex beneath a shallow water column (~90-130m) and provides a good test area in terms of controlled source electromagnetic (CSEM) surveying. Towed streamer EM data acquired in October 2012 show strong EM anomaly over the BBK structures. Using a realistic reservoir model interpreted from seismic data improved the EM modeling results to interpret the measured anomaly. Introduction of non-HC related high-resistivity elements provides more realistic EM modeled responses. The measured data were inverted as a series of 1D inversion for all common mid-points (CMP) along two survey lines to produce transverse resistance, which correspond fairly well with seismically interpreted high-resistivity structures. EM modeled data also indicates that resistive structures can be interpreted even when seismic interpretation is challenging and thus measured EM data can complement seismic data in structural model building. The two techniques integrated together hence provide a more powerful methodology than either technique alone.

Introduction

As part of a larger acquisition campaign in October 2012 we acquired high quality CSEM data, using a Towed Streamer EM system, in the BBK area; see Figure 1 for location and data coverage for the BBK area EM survey lines. 3D dual sensor seismic data acquired over BBK in 2011 were utilized to delineate subsurface structures (Figure 1), and to build the models (Figure 3). Also shown are the available well-log data (black markers in Figure 1).

Towed streamer EM data were acquired utilizing a bi-pole source (800 m long) towed at 10m below sea level and streamer based EM sensors towed simultaneously at a nominal depth of 50m. The source-signal sequence is 120s long with the active (runs at 1500 amperes) 90s followed by 30s no signal (used for background noise estimation and noise reduction processing). The EM streamer has effectively 44 offsets varying from 50 – 7,500m. The towing speed was 4–5 knots.

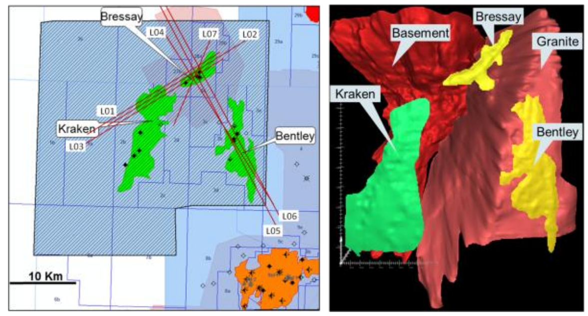

Figure 1: The survey area of the data acquisition showing the Bentley, Bressay and Kraken (left), and the main structural units interpreted from seismic data for 3D structural resistivity model of the BBK area used to design the acquisition, and to provide a reference for the interpretation (right). Red lines indicate EM survey lines.

The processing consists of de-convolving the measured electric field with the output source current to obtain the frequency responses for all available offsets, frequencies and shot points, and application of noise reduction algorithms (Mattsson et al., 2012). In this study we used data at the frequency range of 0.2-3.0 Hz.

A key part of a CSEM project is the forward modeling, especially in complex geological areas where there is likely to be resistive geology that is not associated with hydrocarbon accumulations. A significant issue is deciding how much complexity to include in any model of the sub-surface: we use a step-wise approach to EM model building where the impact of different geological units on sensitivity to a resistive hydrocarbon target is assessed. We use forward modeling to investigate how integrating realistic subsurface resistivity structures interpreted from seismic data can improve the EM data analyses and to improve both the model, and the subsurface interpretation.

The intrusive granite beneath the Bentley discovery has generally been interpreted as regionally persistent (Underhill, 2001, Holloway et al., 1991), but our interpretation of the dual streamer seismic data provides a more precise definition of the lateral extent of the granite. By contrast the weakness of the seismic reflections within the Kraken reservoir makes structural interpretation challenging and here EM surveys are of assistance. 1D differential evolution (DE) inversion was performed to

DOI http://dx.doi.org/10.1190/segam2013-1409.1

explain the resistivity anomaly modeled from seismically interpreted subsurface structures.

Towed Streamer EM data

Processed data along survey lines L03 (over Bressay and Kraken structures) and L04 (over Bressay and Bentley) are shown in Figure 2. The data are presented as the amplitude and phase over a broad range of offsets (943-7457m) and frequencies of 0.4 and 1.8 Hz, respectively. The data quality is good with stable amplitude and phase estimates over a broad frequency and offset range (overall total uncertainties of the data are <5%). The frequency responses shown have a number of features that persist from line to line. For example, the phase at intermediate-long offsets (3000-6000m) and frequencies (0.4-1.8 Hz, the examples shown) vary by about 40-50 degrees along the lines shown. Also, at higher frequencies and shorter offsets the amplitude and phase vary smoothly along the line, with isolated data anomalies.

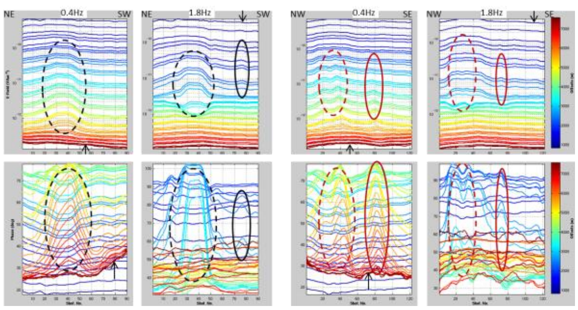

Figure 2: Example of a frequency response amplitudes (upper panel) and phases (lower panel) for a broad range of offsets (943 to 7457m) for survey lines L03 and L04. The shot number is a proxy for position along the survey lines: each position is separated by about 250m. Down-arrows indicate bathymetry trends, whereas up-arrows indicate possible trend of deeper anomaly. Ellipses show possible local anomalies at intermediate offsets (2000-5000m). Dashed-line ellipses represent the location of Bressay, whereas the black and red ellipses indicate the location of Kraken and Bentley structures.

EM modeling

We use the seismic data to construct sub-surface structural models. From the seismic interpretation, the reservoir volumes (Figure 3) are modeled using the well tops and uniform Oil-Water Contacts (OWCs). Top granite is ~1500 m below sea-level, but the base is not clearly defined in the seismic data and in this study, base granite is modeled at 2000m below seabed. It is more sophisticated to model using both topography and areal extent to provide a more constrained thickness. The modeled survey lines are taken from the EM multi-client survey in ESP to replicate real acquisition (Figure 1). The well log data are used to assign resistivity within the structural models.

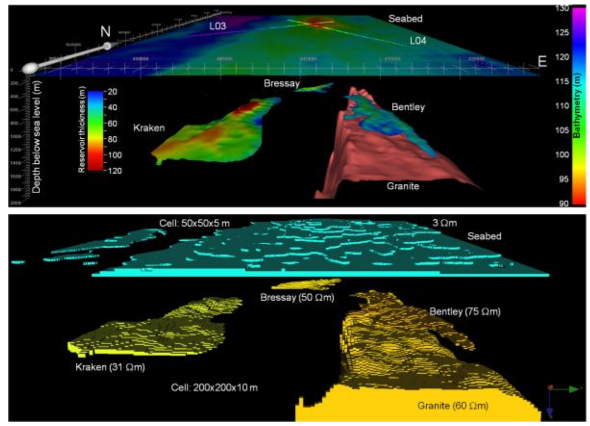

Figure 3: Upper panel shows the bathymetry varying from 90 to 125 m below sea level with corresponding EM shot-points along survey lines L03 and L04. Also showing thickness of Bentley, Bressay and Kraken reservoirs located at the interval between 1000–1270 m below sea level. Depth of the granite intrusion is approximately 1500 m below sea level. Lower panel shows the 3D structure-resistivity grids used in forward modeling.

There are many benefits in making the maximum use of all geophysical data, and geophysical and geological knowledge, as inputs into the Towed Streamer EM scenario model. Towed Streamer EM forward modeling comprises stepwise progressions from simple plane-layer through to complex scenario modeling using realistic reservoirs and other structural units. Each step is evaluated in the context of EM sensitivity to subsurface resistivity contrast before moving to the next level of complexity. A very important aspect of the evaluation is the use of knowledge-based analysis in the acceptance or rejection of a model – in essence making constant reality checks.

The target responses are the normalized frequency response magnitudes and phase differences referred to an off-target measurement (Mattsson et al., 2010). The study focuses mainly on normalized frequency response magnitudes.

Measured target responses for both the survey lines over the Bressay reservoir are significantly strong (~200% normalized frequency response magnitudes) at offsets 4000m (right panel in Figure 4) for frequency ~0.4 Hz. The strong EM anomaly at offsets 2500-4000m may represent the target depth ~1200m below seafloor correspond to the seismically interpreted depth of the Bressay reservoir. However, the response over Bressay might be enhanced due to water depth variation along the survey lines (shallowest over Bressay). Here we compare the measured responses with the modeled ones (lower-right, Figure 4).

DOI http://dx.doi.org/10.1190/segam2013-1409.1

When compared to modeled data we found a larger measured EM anomaly over Bressay but a weak anomaly over Kraken. This could be due to overestimated resistivity and/or thickness for the Kraken reservoir and underestimated lateral extent for the Bressay reservoir. This indicates that measured EM data can complement structural model building. Measured data can also be affected by strong bathymetry over Bressay structures along survey line L03. This will be addressed in the next phase of interpretation.

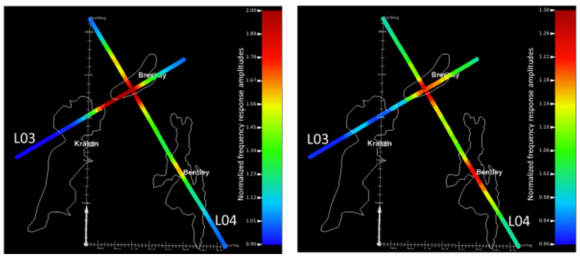

Figure 4: Measured (left) and modeled (right) normalized frequency response amplitudes along survey lines L03 and L04 at an offset of 4000m at 0.4 Hz.

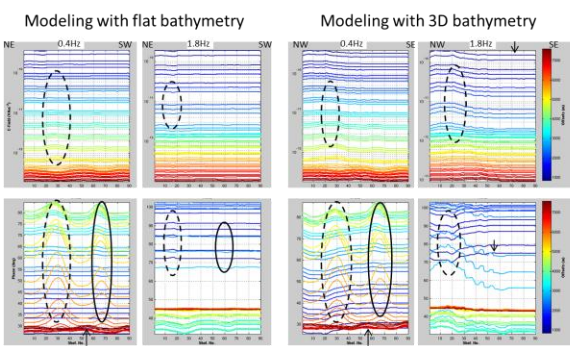

Figure 5: Modeled frequency response amplitudes (upper panel) and phases (lower panel) for offsets of 943- 7457m along survey line L03. The shot number is a proxy for position along the survey lines: each position is separated by about 250m. Down-arrows indicate bathymetry trends, whereas up-arrows indicate possible deeper anomaly. Ellipses show local anomalies at intermediate offsets (2000-5000m). Modeled responses improved by introducing 3D bathymetry here (right).

Figure 5 shows how introducing the 3D bathymetry model improves the modeled data along survey line L03. Measured data shows a strong bathymetry trend towards SW direction at high-frequency and short-offset combination (down arrow in Figure 2, left panel). Modeled data for reservoir structures embedded in flat bathymetry provides monotonous response at high-frequency and short-offset combination (Figure 5, left panel). After introducing the 3D bathymetry layer the modeled data show the similar trend (down arrow in Figure 5, right panel) as observed in the measured data.

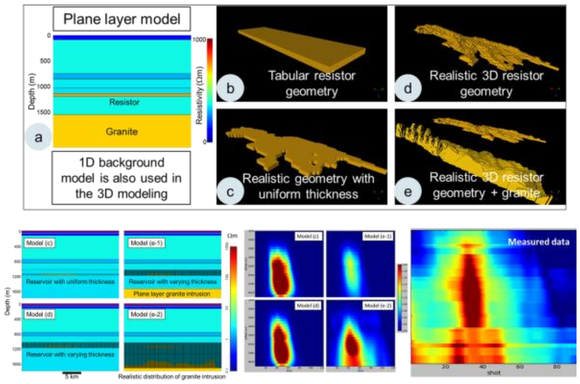

Figure 6: Structural-resistivity models (upper panel). Lower panel shows modeled resistivity sections (left) modeled EM target responses (middle) and measured responses (right). Modeled response improved by introducing granite below Bentley structure.

Line L04 covers various structural complexities including the Bentley reservoir, the Balder tuff layer and the granite intrusion. This line has been modeled using several progressive scenarios to capture the impact of the geological complexities. Vertical sections in Figure 6 show how this complexity changes. The target response for a plane-layer model (model (a)) is unrealistically high and excluded from the display. Modeled response for a 3D box model (model (b)) is overestimated laterally (not shown) and the response for a realistic model (model (c)) with uniform thickness is also overestimated at the edge. However, the response for a 3D realistic reservoir model without granite intrusion (model (d)) is strong at long offsets; which should be influenced by the granite intrusion. A plane-layer granite intrusion (model (e-1)) reduces the overall target response which is then substantially improved by introducing a 3D granite intrusion (model (e-2)). In terms of morphology, modeled responses for scenario e-2 are closest to the measured data (lower-right) and hence the scenario, e-2 is the preferred reference model from this restricted set. However, the modeled background resistivity is required to be increased to achieve a shorter offset anomaly comparable to the measured one (offsets 2000 -5500m in measured data).

Resistivity estimation

In order to recover the subsurface resistivity EM frequency responses along survey lines, L03 and L04 were used as input to the 1D DE inversion scheme (a population based stochastic function minimizer) after Storn and Price, 1997. We performed the inversion in the frequency domain, where the data for a number of frequencies (0.2, 0.4, 0.6, 0.8 and 1.0 Hz) and offsets (2700-7450m, with an interval

DOI http://dx.doi.org/10.1190/segam2013-1409.1

of about 250m) are used simultaneously. The minimizing objective function is the root means squared difference between the measured and the modeled data,

$$\chi^2 = \sum_{\substack{freqs\\ offsets}} \frac{(E^{\mathrm{Re}}_{\mathrm{mod}} - E^{\mathrm{Re}}_{meas})^2 + (E^{\mathrm{Im}}_{\mathrm{mod}} - E^{\mathrm{Im}}_{meas})^2}{|E_{meas}|^2}$$

where E_{meas} is the measured electric field data, E_{mod} is the modeled data and χ is the misfit.

Measured frequency responses are sorted to the CMP bins and 1D DE inversion recovers the resistivity for individual CMP locations along the survey lines. The inverted resistivity models were then stitched together to form a 2D resistivity section along the survey lines. At first the background resistivity was recovered through two layered (water and half-space) inversion while the water conductivity and depth of the seabed (echo-sounder bathymetry at CMP positions) remain fixed. In this case, the seawater is approximated as one layer with a resistivity of 0.259 ohm-m taken from a conductivity, temperature & depth (CTD) measurements. The low frequency (< 1 Hz) and intermediate to large offset (> 2700 m) data (less affected by the shallow inhomogeneity and the targets) are selected in this step.

In the second step, we constrained the inversion assuming a three-layered half-space below seabed: the over-burden (above the regional base Balder Tuff layer), the target-layer (between base Balder Tuff and Base Cretaceous Unconformity (BCU)) and the under-burden (below BCU). The resistivities in the over-burden and the target layers are unconstrained whereas the water layer and the under-burden were fixed to the recovered background resistivity in the first step. The water depth is estimated from echo sounder measurements on board the vessel. The water depth varies from 90 to 130m.

Even though shorter offsets are available in the dataset, they are neglected in the data going into the inversion. The reason is that a more finely resolved structure based on seismic data is needed to capture the variations in these short offsets. However, to characterize the deeper anomaly region and to roughly estimate the overburden, the set of offsets from 2700 – 7450m is sufficient. The selected frequency range is chosen to be sensitive to the anomaly region but also sufficient to be able to estimate both the vertical and horizontal resistivities in the four layer thick model.

The resulting transverse resistance for the target layer is shown in Figures 7 for line L03 and L04. The strong responses on survey line L04 correspond well with the field outlines and the modeled data for the Bentley and Bressay reservoirs. The response south-west on line L03 is higher than expected. This could be explained by the fixed resistivity used as the input to the inversion for the under-burden. Varying amplitudes and phases towards south-west at a long-offset/low-frequency combination along L03 indicate a deeper regional anomaly (Figure 2, left panel). The influence of the resistivity in the under-burden may have been underestimated for line L03, particularly at the south-west part.

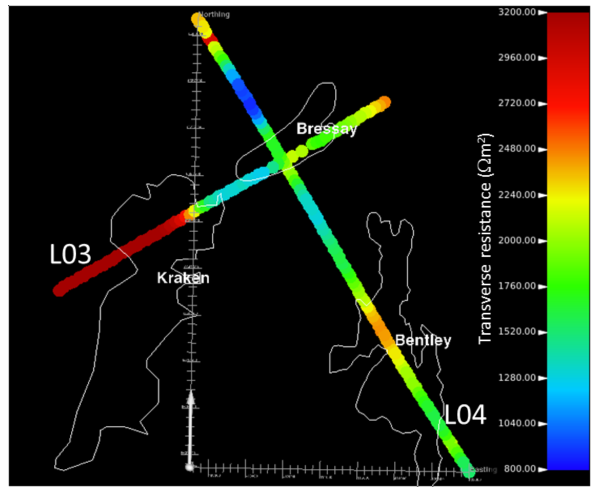

Figure 7: Inverted transverse resistance for line L03 and L04.

Conclusions

Using a realistic reservoir model interpreted from seismic data (Bressay, Bentley and Kraken) improved the EM modeling results. Introduction of non-HC related high-resistivity elements (the granite intrusion and Balder Tuff layer) provides more realistic EM modeled responses. The delineation and interpretation of Kraken reservoir was challenging due to the lack of clarity in the seismic reflection data. EM modeled data indicates that resistive structures can be interpreted even when seismic interpretation is challenging and thus measured EM data can complement seismic data in structural model building. The two techniques integrated together hence provide a more powerful methodology than either technique alone. Inversion results correspond well with the seismically interpreted structures along survey line L04. The discrepancies observed along L03 could possibly be improved by implementing 3D inversion as a further scope of studies with the dataset.

Acknowledgements

The authors acknowledge PGS for giving permission to show the data.

http://dx.doi.org/10.1190/segam2013-1409.1

EDITED REFERENCES

Note: This reference list is a copy-edited version of the reference list submitted by the author. Reference lists for the 2013 SEG Technical Program Expanded Abstracts have been copy edited so that references provided with the online metadata for each paper will achieve a high degree of linking to cited sources that appear on the Web.

REFERENCES

Mattsson, J., L. Lund, and J. Lima, 2010, A towed EM system for hydrocarbon exploration tested on a gas discovery in the North Sea: EGM 2010 International Workshop.

Mattsson, J., P. Lindqvist, R. Juhasz, and E. Björnemo, 2012, Noise reduction and error analysis for a towed EM System: 82nd Annual International Meeting, SEG, Expanded Abstracts, http://dx.doi.org/10.1190/segam2012-0439.1.

Holloway, S., D. Reay, J. A. Donato, and B. Beddoe-Stephens, 1991, Distribution of granite and possible Devonian sediments in part of the East Shetland Platform, North Sea: Journal of the Geological Society, **148**, no. 4, 635–638, http://dx.doi.org/10.1144/gsjgs.148.4.0635.

Storn, R., and K. Price, 1996, Minimizing the real functions of the ICEC'96 contest by Differential Evolution: IEEE Conference on Evolutionary Computation, Nagoya. 842–844.

Underhill, J. R., 2001, Controls on the genesis and prospectivity of Paleogene palaeogeomorphic traps, East Shetland Platform, UK North Sea: Marine and Petroleum Geology, **18**, no. 2, 259–281, http://dx.doi.org/10.1016/S0264-8172(00)00067-2.